Sequence of Events for the Formation of Titanate Nanotubes, Nanofibers, Nanowires, and Nanobelts

Di Wu,* Ji Liu, Xiaoning Zhao, Aidong Li, Yanfeng Chen, and Naiben Ming

National Laboratory of Solid State Microstructures and Department of Materials Science and Engineering, Nanjing University, Nanjing 210093, China

Received August 24, 2005. Revised Manuscript Received November 15, 2005

The formation of $H_2Ti_3O_7$ nanotubes, nanofibers, nanowires, and nanobelts via alkali hydrothermal synthesis was studied in detail by TEM and HRTEM. The effects of preparation parameters, such as reaction temperature, duration, and cooling process, on the morphologies of the products are clarified. A universal formation mechanism is proposed based on the growth, split, wrapping, and thickening of $Na_2Ti_3O_7$ nanointermediates, which links all kinds of morphologies observed for $H_2Ti_3O_7$ nanoentities.

Introduction

In recent years, one-dimensional nanostructures have attracted much attention due to their potential applications in a variety of novel devices.[1−4] The most prominent example is certainly the carbon nanotubes.[1−3] Considerable efforts have been spent on the synthesis of nanotubes or nanowires of more complex structures. A particularly significant breakthrough was made by Tenne and co-workers to synthesize chalcogenide nanotubes by reduction of needlelike metal oxide crystals with H_2 and H_2S.[5,6] Various approaches to other one-dimensional nanomaterials including metals,[7] oxides,[8] and nitrides[9] have also been reported. It was noticed that the class of oxidic nanotubes and nanowires might offer many properties and advantages leading directly to new technological applications, such as nanoelectronics and nanophotonics.[10,11] Oxidic nanotubes and nanowires can be achieved in either gas- or solution-based methods. Carbon nanotubes or anodic alumina oxide may also be used as templates to direct the growth.[12] An important approach to oxidic nanowires and nanotubes is the hydrothermal or solvothermal synthesis that provides access to uniform and distinct morphologies in large scales with remarkable reliability, selectivity, and efficiency.[13]

Among the one-dimensional oxidic nanomaterials reported, titanium oxide is of particular interest for its wide applications as catalyst supports,[14] semiconductor photocatalysts,[15] and sensors.[16] Titanate nanotubes of ∼8 nm in diameter were first reported by Kasuga and co-workers, employing a hydrothermal treatment of rutile TiO_2 powders in strong aqueous solution of NaOH at 110 °C followed by HCl washing.[17] These authors claimed that the tubular products obtained were of anatase TiO_2 and were formed during the washing procedure.[18] After this, a number of papers were published on the structure and formation of hydrothermally synthesized titanium oxide nanotubes. However, the conclusions of these reports are quite controversial. Du et al.[19] obtained nanotubes by a hydrothermal process at 130 °C, similar to that reported by Kusaga but without washing. Chen et al.[20] concluded that these nanotubes were of $H_2Ti_3O_7$ structure based on diffraction and high-resolution transmission electron microscopy (HRTEM) results. Yang et al.[21] argued that the resulting nanotubes are of $Na_2Ti_2O_4(OH)_2$, not TiO_2 or $H_2Ti_3O_7$. However, Yao et al.[22] and Wang et al.[23] contradicted the claims of Chen and Yang and tried to establish that the products were of anatase structure and formed by rolling single-layer anatase nanosheets. Zhang et al.[24] carried out ab initio calculations on $H_2Ti_3O_7$ to conclude that the nanotubes were formed by rolling around the [010]

* To whom correspondence should be addressed. E-mail: diwu@nju.edu.cn. Tel: +86-25-83594689. Fax: +86-25-83595535.

(1) Iijima, S. *Nature* **1991**, *354*, 56.
(2) Rao, C. N. R.; Satishkumar, B. C.; Govindaraj, A.; Nath, M. *ChemPhysChem* **2001**, *2*, 78.
(3) Dai, H. *Surf. Sci.* **2002**, *500*, 218.
(4) Huang, M. H.; Mao, S.; Feick, H.; Yan, H.; Wu, Y.; Kind, H.; Webber, E.; Russo, R.; Yang, P. *Science* **2001**, *292*, 1897.
(5) Tenne, R.; Margulis, L.; Genut, M.; Hodes, G. *Nature* **1992**, *360*, 444.
(6) Feldman, Y.; Wasserman, E.; Srolovitz, D. J.; Tenne, R. *Science* **1995**, *267*, 222.
(7) Li, Y. D.; Wang, J. W.; Deng, Z. X.; Wu, Y. Y.; Sun, X. M.; Yu, D. P.; Yang, P. D. *J. Am. Chem. Soc.* **2001**, *123*, 9904.
(8) Urban, J. J.; Yun, W. S.; Gu, Q.; Park, H. *J. Am. Chem. Soc.* **2002**, *124*, 1186.
(9) Wu, Q.; Hu, Z.; Wang, X.; Lu, Y.; Chen, X.; Xu, H.; Chen, Y. *J. Am. Chem. Soc.* **2003**, *13*, 2024.
(10) Arnold, M. S.; Avouris, P.; Pan, Z. W.; Wang, Z. L. *J. Phys. Chem. B* **2003**, *107*, 659.
(11) Law, M.; Sirbuly, D. J.; Johnson, J. C.; Goldberger, J.; Saykally, R. J.; Yang, P. *Science* **2004**, *305*, 1269.
(12) Rao, C. N. R.; Nath, M. *Dalton Trans.* **2003**, *1*, 1.
(13) Patzke, G. R.; Krumeich, F.; Nesper, R. *Angew. Chem., Int. Ed.* **2002**, *41*, 2446.
(14) Matsuda, S. *Appl. Catal.* **1983**, *8*, 149.
(15) Dagan, D.; Tomkiewics, M. *J. Phys. Chem. B* **1993**, *97*, 12651.
(16) Varghese, O. K.; Gong, D.; Paulose, M.; Ong, K. G.; Grimes, C. A. *Sens. Acuators B* **2003**, *93*, 338.
(17) Kasuga, T.; Hiramatsu, M.; Hoson, A.; Sekino, T.; Niihara, K. *Langmuir* **1998**, *14*, 3160.
(18) Kasuga, T.; Hiramatsu, M.; Hoson, A.; Sekino, T.; Niihara, K. *Adv. Mater.* **1999**, *11*, 1307.
(19) Du, G. H.; Chen, Q.; Che, R. C.; Yuan, Z. Y.; Peng, L. M. *Appl. Phys. Lett.* **2001**, *79*, 3702.
(20) Chen, Q.; Du, G. H.; Zhang, S.; Peng, L. M. *Acta Crystallogr. B* **2002**, *58*, 587.
(21) Yang, J.; Jin, Z.; Wang, X.; Li, W.; Zhang, J.; Zhang, S.; Guo, X.; Zhang, Z. *Dalton Trans.* **2003**, *1*, 3898.
(22) Yao, D. B.; Chan, Y. F.; Zhang, X. Y.; Zhang, W. F.; Yang, Z. Y.; Wang, N. *Appl. Phys. Lett.* **2003**, *82*, 281.
(23) Wang, W.; Varghese, O. K.; Paulose, M.; Grimes, C. A.; Wang, Q.; Dickey, E. C. *J. Mater. Res.* **2004**, *19*, 417.

10.1021/cm0519075 CCC: $33.50 © 2006 American Chemical Society
Published on Web 12/21/2005

direction of single-layer $H_2Ti_3O_7$ peeled off from $H_2Ti_3O_7$ crystal plates possibly due to hydrogen deficiency in surface layers. However, Bavykin et al.[25] recently proposed that the tubular morphology observed is a result of wrapping of multilayer nanosheets of $H_2Ti_3O_7$ due to mechanical stress. Along with the controversy on composition and formation mechanism, nanoentities with distinctively different morphologies, such as nanotubes, nanofibers, and nanobelts, have been reported with some apparently similar hydrothermal procedures.[25−28] Meanwhile, these nanoscale oxides have shown potential applications in catalysis[29,30] and Li-ion exchange.[31,32]

It is thus important to reveal the effects of synthetic parameters on the morphologies and to clarify the structural relations among different morphologies. A recent endeavor on this aspect is given by Ma et al.[33] employing Raman, X-ray and electron diffraction, and X-ray absorption fine structure. However, high-resolution structure analysis on individual nanoentities, from which the exact sequence of events can be deduced, has not been found in the literature. In this report, we present detailed transmission electron microscopy (TEM) studies on the morphology and structure of nanotubes, nanowires, nanofibers, nanobelts, and intermediate products from hydrothermal treatment of amorphous titanium oxide powders in NaOH aqueous solution at different temperatures. It is observed that not only reaction temperature and duration but also cooling and washing processes have a great impact on the resultant morphology. The results confirm that the structures of resultant nanoentities are related to monoclinic layered titanate $H_2Ti_3O_7$. The structure relations among nanotubes, nanowires, nanofibers, and nanobelts are elucidated. A universal formation mechanism is proposed based on the growth, split, wrapping, and thickening of $Na_2Ti_3O_7$ nanointermediates.

Experimental Section

The starting chemicals used were A. R. reagents from Beijing Chemical Factory without further purification. The amorphous titanium oxide powders were synthesized as follows: 0.08 mol of $TiCl_4$ was diluted into 40 mL of chilled deionized water with constant stirring; $NH_3{\cdot}H_2O$ was added to the clear solution drop by drop and white precipitates appeared; the precipitates were filtered and washed by a large volume of deionized water until the pH value of washing solution reached 7.0; the amorphous powders were then dried at 70 °C overnight. For a typical synthesis of titanate oxide nanostructures, 100 mg of amorphous titanium oxide powders was put into 20 mL of 10 M NaOH aqueous solution, transferred to a Teflon-lined stainless steel autoclave, and sealed. The autoclave was put into an oven, heated to 130−180 °C for prescribed periods of time, and cooled naturally in air. The products were collected, washed with deionized water to a pH value of 7.0, and finally dried at 70 °C overnight. The morphology, size, and structure of titanium oxide nanostructures were characterized using a FEI Tecnai F20 transmission electron microscope operating at 200 keV. For TEM observations, a small amount of products were ultrasonically dispersed in alcohol and deposited on copper grids coated with ultrathin carbon films.

Nomenclature of the nanostructures discussed in this article is listed as follows: lamellar structures are those layered structures grown on the brim of raw TiO_2 particles, appearing at the initial stage of the reaction; nanosheets, which may roll into nanotubes, are formed by splitting these lamellar structures between (100) planes; nanobelts refer to thick nanosheets that cannot roll into nanotubes; nanotubes, nanofibers, and nanowires are used as commonly used in the literature.

Results and Discussion

The morphology evolution of hydrothermal treatment of amorphous titanium oxide powders at 130 and 180 °C is displayed in Figure 1. The starting amorphous powders aggregates to clusters of a few hundreds of nanometers in size (Figure 1a). The amorphous nature is demonstrated by the ring patterns in selected area electron diffraction (SAED) from these powders, as shown in the inset of Figure 1a. After 10 h of hydrothermal treatment at 130 °C, lamellar structures, less than 100 nm in lateral size, are observed around the brim of amorphous powder clusters (Figure 1b). These lamellar structures grew as reaction time increased, as evidenced in the sample after 20 h of hydrothermal treatment (Figure 1c). The lateral size of the lamellar structures increase to around 200 nm. Along with lamellar structures, some tubular nanostructures can also be observed after 20 h of reaction.

The lamellar structures were observed frequently as reported in the literature concerning the formation of titanium oxide nanotubes. Although the top/bottom surface of these lamellar structures was considered to be the (010) plane of anatase TiO_2 [22,23] or (100) plane of monoclinic $H_2Ti_3O_7$ in the literature,[20,24] no direct evidence has been shown to support these speculations. Figure 2 shows an HRTEM image of a typical lamellar structure at the brim of an amorphous powder cluster. Two sets of lattice fringes with periods of 0.21 and 0.31 nm, respectively, are clearly resolved. However, in contrast to those proposed in the literature, these two sets of lattice fringes are not perpendicular to each other, but with an angle around 102°. The periodicity shown in Figure 2 is in agreement with lattice spacing of (800) and (003) crystalline planes of monoclinic layered titanate $H_2Ti_3O_7$ ($C2/m$, $a = 1.603$, $b = 0.375$, $c = 0.919$ nm, $\beta = 101.47°$).[31] The top/bottom surface of the lamellar structures is the (010) plane of $H_2Ti_3O_7$ and the incident electron beam was along the [010] direction. The *a* axis is expanded about 8% compared with $H_2Ti_3O_7$ prepared with conventional ion exchange.[34] This may be ascribed to H_2O molecules inserted into interlayer spaces of layered $H_2Ti_3O_7$.[35] The observation

(24) Zhang, S.; Peng, L. M.; Chen, Q.; Du, G. H.; Dawson, G.; Zhou, W. Z. *Phys. Rev. Lett.* **2003**, *91*, 256103.
(25) Bavykin, D. V.; Parmon, V. N.; Lapkin, A. A.; Walsh, F. C. *J. Mater. Chem.* **2004**, *14*, 3370.
(26) Yuan, Z. Y.; Colomer, J. F.; Su, B. L. *Chem. Phys. Lett.* **2002**, *363*, 362.
(27) Yuan, Z. Y.; Su, B. L. *Colloid Surf. A* **2004**, *241*, 173.
(28) Meng, X. D.; Wang, D.-Z.; Liu, J.-H.; Zhang, S.-Y. *Mater. Res. Bull.* **2004**, *39*, 2163.
(29) Lin, C.-H.; Chien, S.-H.; Chao, J.-H.; Sheu, C. Y.; Cheng, Y.-C.; Huang, Y.-J.; Tsai, C.-H. *Catal. Lett.* **2002**, *80*, 153.
(30) Tokudome, H.; Miyauchi, M. *Chem. Lett.* **2004**, *33*, 1108.
(31) Zhou, Y.-K.; Cao, L.; Zhang, F.-B.; He, B.-L.; Li, H.-L. *J. Electrochem. Soc.* **2003**, *150*, A1246.
(32) Armstrong, A. R.; Armstrong, G.; Canales, G.; Garcia, R.; Bruce, P. G. *Adv. Mater.* **2005**, *17*, 862.
(33) Ma, R.; Fukuda, K.; Sasaki, T.; Osada, M.; Bando, Y. *J. Phys. Chem. B* **2005**, *109*, 6210.

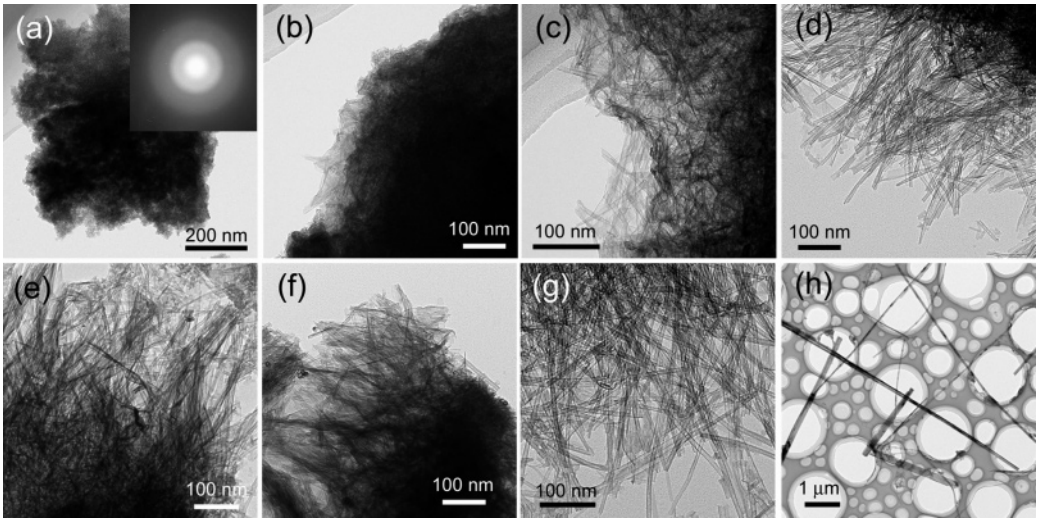

Figure 1. Morphology evolution sequence of $H_2Ti_3O_7$ nanotubes and nanowires as different reaction temperatures and durations were employed. (a) Morphology of as-prepared amorphous TiO_2 powders used as raw materials in the preparation of $H_2Ti_3O_7$ nanoentities. (Inset) SAED pattern indicating the amorphous nature of these powders. (b) Morphology of products after 10 h of reaction at 130 °C. Although a large amount of residual amorphous TiO_2 powders is obvious, thin lamellar structures appeared at the brim of these amorphous powders. (c) Lamellar structures grown and tubular products appeared after 20 h of reaction at 130 °C. (d, e) Abundant nanotubes of several hundreds of nanometers in length appeared after reactions at 130 °C for 30 and 40 h, respectively. (f) Nanotubes appeared after only 10 h of reaction at 180 °C. (g) After 30 h of reaction at 180 °C, high-purity nanotubes were obtained by almost complete consumption of amorphous TiO_2 powders. (h) High-purity nanowires were observed after 40 h of reaction at 180 °C.

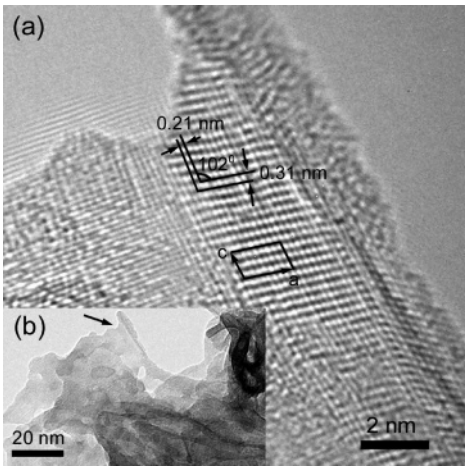

Figure 2. (a) HRTEM image of a typical lamellar structure, showing lattice fringes corresponding to the (010) plane of monoclinic $H_2Ti_3O_7$. (b) Low-magnification image of the lamellar structure at the brim of an amorphous TiO_2 powder, on which the arrow indicates the area magnified in (a).

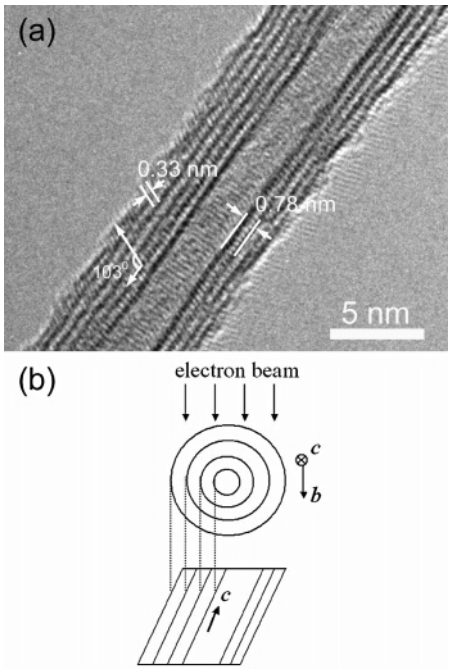

Figure 3. (a) HRTEM of an individual $H_2Ti_3O_7$ nanotube of about 10 nm in diameter, exhibiting an apparent hollow core of about 3 nm in diameter, the asymmetric number of layers at the two sides and lattice fringes corresponding to the (010) plane of monoclinic $H_2Ti_3O_7$ on tube walls. The tube axis is along the [001] direction. (b) A schematic drawing depicting how the lattice image was projected. Concentric configuration for nanotubes is drawn only for simplicity.

of $H_2Ti_3O_7$ lamellar structures indicates that the final nanotubes may probably be of layered $H_2Ti_3O_7$ as well, as noticed earlier by Du et al.,[19] Chen et al.,[20] and Zhang et al.[24] However, the formation mechanism of nanotubes by rolling (100) monolayers of $H_2Ti_3O_7$ around the [010] direction proposed by these authors is questioned since the [010] direction is normal to the observed lamellar structures and thus rolling along this direction cannot result in nanotubes as long as several hundreds of nanometers as observed.

A large amount of nanotubes were observed after 30 h of hydrothermal treatment at 130 °C, as shown in Figure 1d. Most of the nanotubes observed are about 10 nm in outer diameter and more than 300 nm in length. It is interesting to find that the majority of the nanotubes point out from the amorphous titanium oxide powder clusters with one end adhering on them. This is also in agreement with earlier reports using crystalline TiO_2 as precursors.[17,29] A typical HRTEM image of an individual nanotube is shown in Figure 3. The structure of the nanotube is identical to nanotubes obtained using crystalline TiO_2 as the starting materials. The wall thickness of the tube is asymmetric, having five layers on one side and three layers on the other. This indicates that the tubes may probably be formed by scrolling conjoined multilayer nanosheets.[25] The interlayer spacing of these

(34) Feist, T. P.; Davies, P. K. *J. Solid State Chem.* **1992**, *101*, 275.
(35) Suzuki, Y.; Yoshikawo, S. *J. Mater. Res.* **2004**, *19*, 982.

nanotubes is 0.78 nm, close to the value reported in the literature.[20,22] Another set of fringes in Figure 3 is about 103° to the tube axis with a spacing of 0.33 nm. This angle is close to the angle β of monoclinic $H_2Ti_3O_7$. One may argue that the angle observed could be the chiral angle, which is widely observed in carbon nanotubes and can vary in values. However, titanate nanotubes are not formed by rolling large monolayer nanosheets as in the case of carbon nanotubes. It is also noted that the cross section of these nanotubes is "onion" shaped.[25] If the nanotubes are formed by rolling rectangular multilayered nanosheets, the width of the nanosheets should be roughly equal to the perimeter of the nanotubes cross section, about 30 nm, and the length of the nanosheets should be the length of the nanotubes, about 300 nm. Since the lamellar structures grow faster along the [001] direction, the length of the nanosheets should along the [001] direction. Thus, a large chiral angle may result in steps, of a few layers high, on the outer surface of these nanotubes, or form broken tubes. However, HRTEM results show that the outer surface of all the nanotubes is smooth and complete: neither steps nor broken areas are observed. We thus conclude that the nanotubes observed are achiral and the angle observed is the angle β of monoclinic $H_2Ti_3O_7$. This is supported by the observed periodicities of 0.78 and 0.33 nm, close to those of (200) and (003) planes of $H_2Ti_3O_7$ as observed for the lamellar structures (Figure 2a), except a small distortion. Therefore, the incident electron beam should be along the [010] direction on the tube walls. These observations also suggested that the tube axis of these nanotubes should be along the [001] direction of monoclinic $H_2Ti_3O_7$. Figure 1e shows the morphology of the products hydrothermally treated for 40 h at 130 °C. It is similar to that observed for samples treated for 30 h. Hydrothermal treatment at 180 °C may accelerate the reaction. Tubular products appeared after only 10 h of treatment (Figure 1f). And after 30 h of reaction, more than 90% of the products was $H_2Ti_3O_7$ nanotubes with almost all amorphous titanium oxide precursor clusters consumed (Figure 1g).

Hydrothermal treatment longer than 40 h at 180 °C results in a distinctly different morphology. As shown in Figure 1h, amorphous precursor powders have been transformed into nonhollow nanowires with a large size distribution both in length and in diameter. Approximately, the lengths are between several micrometers to about 30 μm and the diameters are between 20 nm to about 200 nm. Thick nanowires are straight due to their rigidness but thin nanowires are flexible and are found to be curved. These nanowires exhibit rectangular cross sections as observed by tilting the sample. A typical HRTEM image is shown in Figure 4a and the corresponding low-magnification bright field image is shown in Figure 4b. The clearly resolved lattice image indicates that these nanowires were well-crystallized. Two sets of lattice fringes at an angle of 102° were resolved with spacing of 0.97 and 0.31 nm, close to the lattice spacing observed for the lamellar structures and nanotubes, corresponding to (200) and (003) planes of $H_2Ti_3O_7$. These nanowires are all found to grow along the [001] direction. Along the *a* axis, the periodically appeared bright and dark contrast corresponds to the "stepped" layered structure of

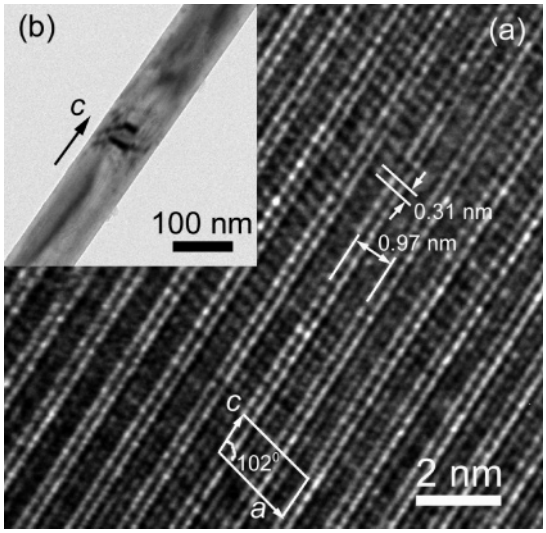

Figure 4. (a) HRTEM of an individual $H_2Ti_3O_7$ nanowire, exhibiting a well-resolved two-dimensional lattice corresponding to the (010) plane of monoclinic $H_2Ti_3O_7$. (b) Low-magnification image of the nanowire. The nanowire grows along the [001] direction.

$H_2Ti_3O_7$.[34] However, the *a* axis spacing of the nanowire is increased by about 10% compared with that observed for the lamellar structures. This further lattice expansion may be caused by more H_2O molecules driven into interlayer spaces of $H_2Ti_3O_7$ structure during prolonged hydrothermal treatment.[35]

It was observed that thin nanowires were formed by splitting $H_2Ti_3O_7$ crystalline sheets between (100) planes, as evidenced in Figure 5. Figure 5a shows a bundle of nanowires splitting from the same root, which, as magnified in the inset, is a piece of crystalline sheet. Figures 5b, 5c, and 5d demonstrate that $H_2Ti_3O_7$ nanowires can further split themselves into thinner ones.

$H_2Ti_3O_7$ is generally proposed to appear in the washing process due to proton exchange of sodium trititanate ($Na_2Ti_3O_7$) formed during autoclaving. It was also proposed earlier that $Na_2Ti_3O_7$ nanotubes were formed by rolling crystalline nanosheets exfoliated from crystalline TiO_2 (anatase or rutile). To support this, thin layers were observed to peel off from precursor titania crystallites after the first few minutes of alkali hydrothermal treatment.[21] If this is true, the length of the nanotubes should be restricted by the size of raw TiO_2 materials since the dimensions of the exfoliated nanosheets are restricted by the size of raw TiO_2 materials. However, we note that the length of the nanotubes obtained is often orders larger than the size of raw TiO_2 particles. For example, Yuan and Su[27] have reported $H_2Ti_3O_7$ nanotubes of several hundreds of nanometers in length derived from TiO_2 particles of 25−30 nm in size; Sun and Li[36] prepared these nanotubes of 300 nm in length using TiO_2 particles about 5 nm in size; and Suzuki and Yoshikawo[35] obtained the same nanotubes approximately 1 μm in length using commercially available Ishihara ST-01 anatase particles, which are reported to be less than 10 nm in size.[37,38]

(36) Sun, X.; Li, Y. *Chem. Eur. J.* **2003**, *9*, 2229.
(37) Sreethawong, T.; Suzuki, Y.; Yoshikawa, S. *J. Solid State Chem.* **2005**, *178*, 329.
(38) Almquist, C. B.; Biswas, P. *J. Catal.* **2002**, *212*, 145.

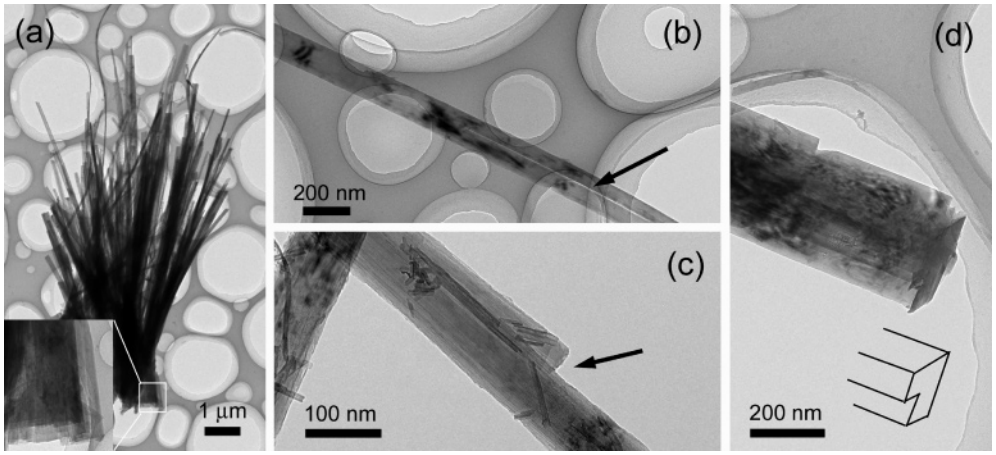

Figure 5. (a) TEM image showing a bundle of $H_2Ti_3O_7$ nanowires splitting from the same root, which was observed to be thick layers as magnified in the inset. (b) A crack developing in the middle of a nanowire about 150 nm in diameter. (c) A step formed by splitting off a thin nanowire from the thick one. (d) A rectangular cross section of a nanowire showing a kink as a result of a thinner nanowire splitting off. The inset is a schematic drawing, which serves as a guide for eyes, illustrating the contour of the cross section.

In contrast to the assumption of nanosheets exfoliation, we propose that raw titania particles were dissolved or partially dissolved in concentrated NaOH solutions followed by $Na_2Ti_3O_7$ nucleation and growth into lamellar structures. We used Co-doped (7.0 mol %) anatase TiO_2 particles as the starting material to prepare nanotubes following the same process: autoclaving in 10 M NaOH at 130 °C for 30 h, thoroughly washing with deionized water, and drying. Composition analysis using inductively coupled plasma spectroscopy shows that Co concentration in the produced nanotubes is only about 4.0 mol %, significantly smaller than that in the starting material. This implies that raw titania was partially dissolved first in concentrated NaOH solutions and then recrystallized into $Na_2Ti_3O_7$, and that TiO_6 octahedra, the building blocks of TiO_2 polymorphs, may probably be the building blocks of produced nanotubes and nanowires.

$Na_2Ti_3O_7$ is composed of corrugated strips of edge-sharing TiO_6 octahedra. Each strip is three-octahedra wide and the strips further corner join to form stepped layers. These Ti−O layers stack in the *a* direction and sodium cations occupy the interlayer positions to form the monoclinic lattice (see Supporting Information SI-1). With the progress of hydrothermal reaction, more and more TiO_2 was dissolved and the concentration of TiO_3^{2-}, $TiO_2(OH)_2^{2-}$, and possible polytitanates $Ti_nO_{2n+m}^{2m-}$ will increase in the solution accordingly. Solid $Na_2Ti_3O_7$ nucleates and grows preferentially at the brim of undissolved TiO_2 particles, as shown in Figure 1b. In a layered compound, the chemical bonding between neighboring layers is generally weaker than chemical bonding in the same layers. Therefore, the growth rate of $Na_2Ti_3O_7$ along the [010] and [001] directions should be faster than that along the [100] direction. As speculated earlier,[19,20,24,25] nanosized $Na_2Ti_3O_7$ should grow into thin layers with (100) planes as the top/bottom surfaces. Thus, $H_2Ti_3O_7$ lamellar structures observed should also have (100) planes as top/bottom surfaces. However, this structure is not in agreement with the observation in the present study (Figure 2a) and not in agreement with nanobelts of a similar compound $H_2Ti_5O_{11}$ reported earlier.[27,39] This phenomenon has not been explained explicitly in the literature. We suggest that one possible reason takes into account that the (100) plane of $Na_2Ti_3O_7$ carries net charges. Therefore, (100) planes contribute extra electrostatic energy to the total free energy of $Na_2Ti_3O_7$ nuclei. The larger the area of the (100) plane, the higher the free energy of the system. Hence, the extending of the (100) plane during growth will be prohibited to reduce the free energy. The morphology observed, with the neutral (010) plane as the dominant surface, is more energetically favored.

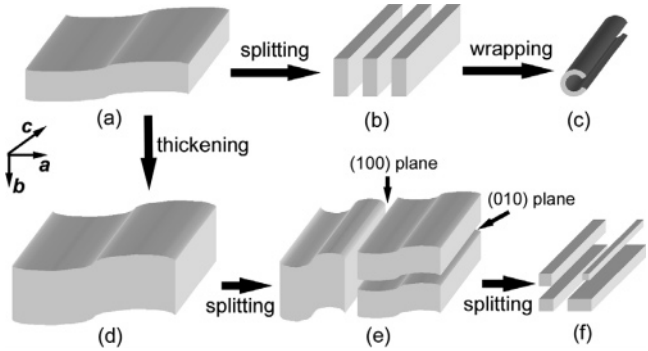

Figure 6. Schematic drawings depicting the formation process of $H_2Ti_3O_7$ nanotubes and nanowires: (a) Lamellar structures grown on the brim of TiO_2 particles. These lamellar structures grow along the [001] direction with the (010) plane as the top/bottom surface. (b) Splitting of lamellar structures into nanosheets between (100) planes. The height of these nanosheet structures (in the *b* direction) is the thickness of the original lamellar structures. (c) Wrapping of nanosheets into nanotubes; the diameter of the nanotubes depends on the height of the nanosheets. (d) Thick layers or wires formed after prolonged reaction at elevated temperature. (e) Splitting of these thick layers or wires between (100) and (010) planes. (d) Further splitting to form thin nanowires.

The thickness of $Na_2Ti_3O_7$ lamellar structures increases as the reaction progresses. After the reaction is terminated, the temperature reduces. During this process, the $Na_2Ti_3O_7$ lamellar structures may split between (100) planes into nanosheets of a few atomic layers in width. This is possible because the chemical interaction between (100) planes is very weak.[24] The resultant nanosheets of $Na_2Ti_3O_7$ will wrap itself around the *c* axis to form nanotubes. The wrapping process was previously proposed to happen in the washing process.[18] However, recent results show that tubular nanostructures can

(39) Yang, H. G.; Zeng, H. C. *J. Am. Chem. Soc.* **2005**, *127*, 270.

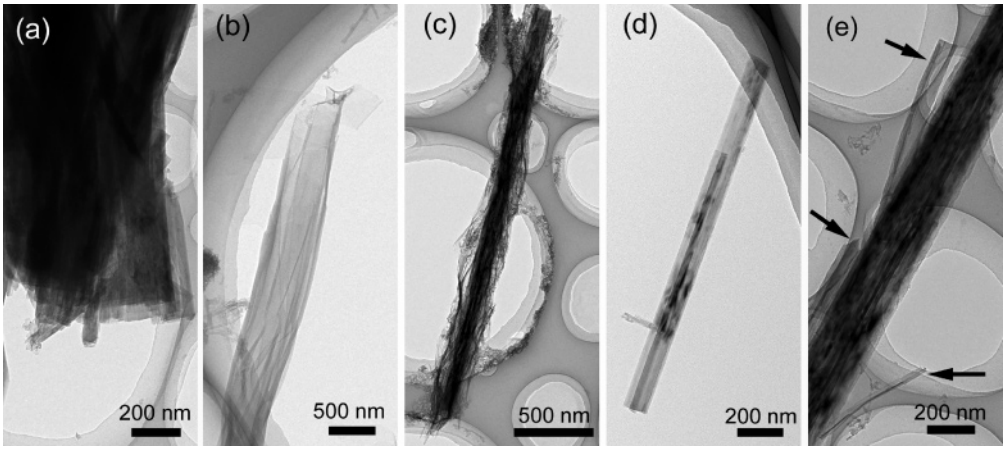

Figure 7. Morphology evolution in the formation of $Na_2Ti_3O_7$: (a) Thick layers, from which nanowires may split off, formed at elevated reaction temperature. (b) Lamellar structures of large areas. (c) Thickening of lamellar structures by growth and by folding themselves. (d) Further condensation to form fibers or nanowires. (e) The surface of a nanowire on a magnified scale, showing lamellar structures on the surface indicated by arrows.

be observed before washing.[19,23,33,40] The driving force for the wrapping may be asymmetry due to preferential doping of these nanosheets with hydrogen together with unsymmetrical surface forces due to locally high surface energy.[22,24,25] As calculated, the gain in surface energy for such a wrapping is enough to compensate mechanical tensions arising due to curving.[24,25] The proposed sequence of events for the formation of titanate nanotubes is depicted in Figures 6a−6c. As reaction temperature increases, the thickness of the initial $Na_2Ti_3O_7$ lamellar structures in the *b* direction (Figure 6a) increases due to enhanced growth rate at elevated temperatures. Therefore, the height of the split $Na_2Ti_3O_7$ nanosheets and the diameter of final $H_2Ti_3O_7$ nanotubes also increase with reaction temperature. This is consistent with those reported earlier. Bavykin et al.[25] found an increase of average nanotubes diameter with increasing temperature from 120 to 150 °C. Lan et al.[40] also reported a double of outer diameters with the increase of reaction temperature from 100 to 150 °C.

At even higher temperatures, the thickness of lamellar structures (Figure 6a) increases more quickly as the reaction time increases. This generates thick layers of $Na_2Ti_3O_7$, as shown in Figure 7a. These thick layers may split between (100) planes of $Na_2Ti_3O_7$ to form nanowires (Figure 5a). Thin lamellar structures of $Na_2Ti_3O_7$ may also condense themselves by folding along the *c* axis to form thick wires directly. This process is recorded in Figures 7b−7d. Such a folding may be driven by decreasing the free energy by reducing the solid/solution interface. Sheetlike structures on the surface of nanowires, which is evidence for this self-folding process, can be frequently observed, as shown in Figure 7e. These thick wires then split between (100) and (010) planes into thinner nanowires[41] by agitation during the cooling or washing process, as depicted in Figures 6d−6f.

It is impossible to observe the morphology change in the hydrothermal autoclave. To verify the formation sequence proposed above, special hydrothermal reaction procedures were designed to interrupt the reaction in different ways.

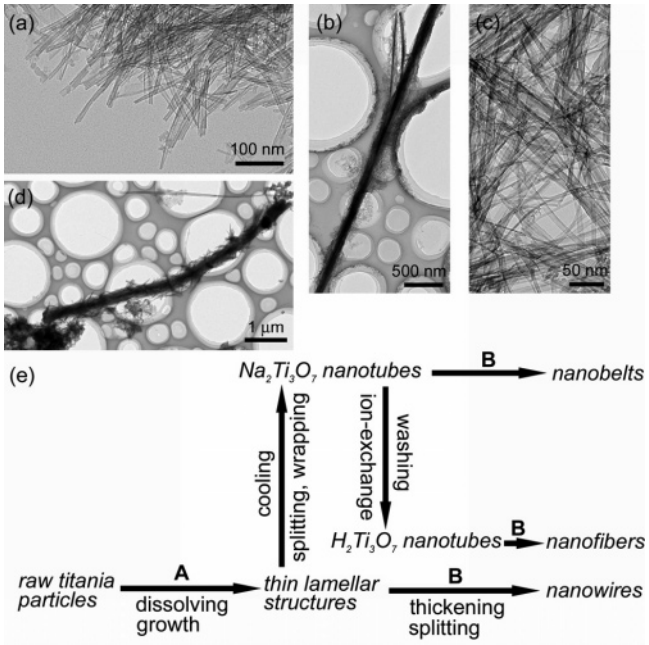

Figure 8. (a) Nanotubes observed after reaction at 130 °C for 30 h. (b) Nanowires observed after reaction at 130 °C for 30 h and 180 °C for 10 h. (c) Nanobelts observed after reaction at 130 °C for 30 h, cool to room temperature and re-reacted at 180 °C for 10 h. (d) Nanofibers observed after reaction at 130 °C for 30 h, cool to room temperature, thoroughly washing and re-reacted at 180 °C for 10 h. (e) Summary of the morphology evolution in (a), (b), (c), and (d): process **A** represents alkali hydrothermal treatment at 130 °C for 30 h and process **B** represents alkali hydrothermal treatment at 180 °C for 10 h.

The morphology of the products were then observed and compared, from which the morphology evolution inside the autoclave can be deduced. Four reactions were conducted and the products were washed and dried by the same process as described earlier. The first reaction was terminated after alkali hydrothermal treatment at 130 °C for 30 h as a control. Nanotubes were observed as shown in Figure 8a. In the second reaction, the autoclave was heated directly to 180 °C for 10 h after the reaction at 130 °C for 30 h. Nanowires were observed as shown in Figure 8b. After the third reaction, in which the autoclave was cooled naturally to room temperature and then heated again to 180 °C for 10 h after the reaction at 130 °C for 30 h, nanobelts were observed as shown in Figure 8c. In the fourth reaction, the products were

(40) Lan, Y.; Gao, X.; Zhu, H.; Zheng, Z.; Yan, T.; Wu, F.; Ringer, S. P.; Song, D. *Adv. Funct. Mater.* **2005**, *15*, 1310.
(41) Wang, R. H.; Chen, Q.; Wang, B. L.; Zhang, S.; Peng, L.-M. *Appl. Phys. Lett.* **2005**, *86*, 133101.

collected after hydrothermal treatment at 130 °C for 30 h, thoroughly washed, and then put into 10 M NaOH solution and autoclaved again at 180 °C for 10 h. This results in nanofibers about 500 nm thick and several micrometers long (Figure 8d). Distinctively different morphologies observed indicate that one may control the morphology of $H_2Ti_3O_7$ nanoentities by interrupting the alkali hydrothermal treatment in different ways. The proposed morphology evolution corresponding to these reactions was summarized in Figure 8e. These observations give evidence that if we do not terminate the reaction and cool the solution at an appropriate stage, nanotubes, as shown in Figure 8a, will not be obtained. Nanowires (Figure 8b) were observed due to the split of thick $Na_2Ti_3O_7$ layers formed by thickening of $Na_2Ti_3O_7$ lamellar structures (formed during 130 °C hydrothermal treatment) in the *b* direction during 180 °C hydrothermal treatment. The increase of thickness is not only a result of capturing monotitanate TiO_3^{2-} and $TiO_2(OH)_2^{2-}$, or polytitanates $Ti_nO_{2n+m}^{2m-}$ from the solution but also a result of self-folding of the lamellar structures. This assumption is supported by observing a large amount of nanowires while putting very few TiO_2 (20 mg) particles into the autoclave (see Supporting Information SI-II). This observation supports the self-folding mechanism because otherwise large areas of thin nanosheets will be kept since the nutrient source is not enough for the growth of $Na_2Ti_3O_7$ into thick layers, from which the nanowires split off. However, if a cooling process is inserted between two alkali hydrothermal treatments, large area thin $Na_2Ti_3O_7$ lamellar structures will split into small pieces of nanosheets and wrap into nanotubes. These $Na_2Ti_3O_7$ nanotubes may be unfolded during subsequent alkali hydrothermal reaction at 180 °C and the thickness of these nanosheets may increase (in the *a* direction of $Na_2Ti_3O_7$) during this subsequent reaction. This increased thickness makes it energetically unfavorable to wrap themselves into tubes. On the other hand, these small pieces of $Na_2Ti_3O_7$ cannot effectively increase their thickness by self-folding. Therefore, nanowires cannot be observed in Figure 8c. A washing process inserted also has effects on the final morphology. Re-autoclaving of $H_2Ti_3O_7$ nanotubes in concentrated NaOH solution at 180 °C results in nanofibers composed of entangled nanosheets, different from nanowires obtained by re-autoclaving $Na_2Ti_3O_7$ nanotubes following the same process. This may represent the influence of chemical composition. Although the mechanism is still unclear at this time, the transformation of $H_2Ti_3O_7$ nanotubes into nanofibers and the transformation of $Na_2Ti_3O_7$ nanotubes into nanobelts demonstrate the metastable nature of the nanotubular morphology in this system.

Summary

In summary, the structures of $H_2Ti_3O_7$ nanotubes, nanofibers, nanowires, nanobelts, and intermediate products prepared by the alkali hydrothermal method were studied in detail using TEM and HRTEM. The microstructure relations among these nanoentities were elucidated. The formation sequence is deduced based on growth, split, wrapping, and thickening of $Na_2Ti_3O_7$ nanointermediates. The significance of this work is 3-fold: (1) the nanotubes were confirmed as a result of wrapping multilayer nanosheets of (100) planes around the *c* axis of $Na_2Ti_3O_7$; (2) the impacts of reaction temperature, duration, and cooling process on the morphology of products were clarified and the exact sequence of events was deduced; and (3) morphology control by adjusting hydrothermal conditions for $H_2Ti_3O_7$ nanoentities is justified.

Acknowledgment. Financial support from National NSF of China (10574067 and 50302003), NSF of Jiangsu province (BK2005415), and State Key Programs for Basic Research of China (2001CB610404) are greatly acknowledged.

Supporting Information Available: Schematic representation of the crystal structure for $Na_2Ti_3O_7$, projected along the [010] direction. Low-magnification TEM image of $H_2Ti_3O_7$ nanowires prepared by reaction of 20 mg of TiO_2 with 20 mL of 10 M NaOH solution (PDF). This material is available free of charge via the Internet at http://pubs.acs.org.

CM0519075